Theor Chem Acc (2004) 112: 282–289
DOI 10.1007/s00214-004-0580-5

Theoretical Chemistry Accounts

Regular article

Homolytic dissociation in hydrogen-bonding liquids: energetics of the phenol O–H bond in methanol and the water O–H bond in water

S. G. Estácio,[1,2] P. Cabral do Couto,[1,2] R. C. Guedes,[1,2] B. J. Costa Cabral,[1,2] J. A. Martinho Simões[1]

[1] Departamento de Química e Bioquímica, Faculdade de Ciências, Universidade de Lisboa, 1749-016 Lisboa, Portugal
[2] Grupo de Física Matemática da Universidade de Lisboa, Av. Professor Gama Pinto 2, 1649-003 Lisboa, Portugal

Received: 18 July 2003 / Accepted: 28 December 2003 / Published online: 29 April 2004

Abstract. The energetics of the phenol O–H bond in methanol and the water O–H bond in liquid water were investigated by microsolvation modelling and statistical mechanics Monte Carlo simulations. The microsolvation approach was based on density functional theory calculations. Optimised structures for clusters of phenol and the phenoxy radical with one and two methanol molecules are reported. By analysing the differential solvation of phenol and the phenoxy radical in methanol, we predict that the phenol O–H homolytic bond dissociation enthalpy in solution is 24.3±11 kJ/mol above the gas-phase value. The analysis of the water O–H bond dissociation by microsolvation was based on optimised structures of $OH^{\bullet}$–$(H_2O)_{1-6}$ and –$(H_2O)_{1-7}$ clusters. Microsolvation modelling and statistical mechanics simulations predict that the HO–H bond dissociation enthalpies in the gas phase and in liquid water are very similar. Our results stress the importance of estimating the differences between the solvation enthalpies of the radical species and the parent molecule and the limitations of local models based on microsolvation.

Keywords: Homolytic dissociation – Density functional theory – Monte Carlo – Hydrogen bonding – Microsoration

1 Introduction

The energetics of the phenol O–H bond in the liquid phase has been analysed in several experimental [1,2,3,4,5] and theoretical works [6,7,8,9]. This subject is of great interest because phenolic compounds play a major role in the chemistry of living organisms, including green plant photosynthesis [10], biocatalysis [11], and protein redox reactions [12]. Moreover, almost all of these processes take place in solution. The energetics of the PhO–H homolytic bond dissociation in solution is defined by the enthalpy of the process:

$$\mathrm{PhOH(sln)} \rightarrow \mathrm{PhO^{\bullet}(sln)} + \mathrm{H^{\bullet}(sln)}, \quad (1)$$

which will be represented by D_{sln}(PhO–H). The enthalpy of the corresponding process in the gas phase will be denoted by D(PhO–H). The recommended experimental value for this quantity is 371.3±2.3 kJ/mol [1]. By evaluating

$$\Delta D = D_{\mathrm{sln}}(\mathrm{PhO-H}) - D(\mathrm{PhO-H}) \quad (2)$$

the importance of solvent effects can be discussed. Some experimental works [3,5] indicated that ΔD should be quite small in hydrogen-bonding liquids, namely around 13 kJ/mol in aqueous solution [3] and around 12 kJ/mol in dimethyl sulphoxide [2]. On the other hand, Wayner et al.[4] predicted that solvent effects on ΔD were much more important. For instance, ΔD was estimated as around 36 kJ/mol in dimethyl sulphoxide. Although these authors have not performed experiments on the hydration of phenol, they predict similar effects in hydrogen-bond acceptor solvents [4]. However, their predictions were based on a local model approach (hydrogen-bond-only), where ΔD was identified with the enthalpy of the hydrogen bond between phenol and one solvent molecule.

Recently, we have analysed the differential hydration of phenol and the phenoxy radical by Monte Carlo simulations [8] and our prediction is that ΔD is around 30 kJ/mol. In the present study we are extending our previous investigation to PhO–H bond dissociation in liquid methanol. Moreover, we have decided to analyse the energetics of the homolytic dissociation of the HO–H bond in liquid water, which is described by the process

$$\mathrm{H_2O(sln)} \rightarrow \mathrm{OH^{\bullet}(sln)} + \mathrm{H^{\bullet}(sln)} \quad (3)$$

The bond dissociation enthalpy of this reaction is represented by D_{sln}(HO–H). The corresponding gas phase value, D(HO–H), has been the subject of numerous investigations (see Ref. [13] and references therein).

Proceedings of the 11th International Congress of Quantum Chemistry satellite meeting in honor of Jean-Louis Rivail

Correspondence to: B. J. Costa Cabral
e-mail: ben@adonis.cii.fc.ul.pt

D(HO–H) is considered a reference quantity owing to the importance of the OH$^\bullet$ radical in many chemical and biochemical processes. One recent evaluation predicts that D(HO–H) = 492.08±0.67 kJ/mol [13]. The generation of the OH$^\bullet$ radical in liquid water by radiolysis has been the subject of several studies [14,15,16,17]. The deleterious effects of the OH$^\bullet$ radical on biological systems are well known [18,19]. In addition, most of the reactions involving this species occur in an aqueous environment; therefore, the energetics of the hydrated OH$^\bullet$ radical is of great interest in many biochemical processes.

The present work is based on two (complementary) approaches: microsolvation modelling and statistical mechanics Monte Carlo simulations. By using the first approach, quantum information on the structure, energetics, and charge distribution of small clusters has been used to discuss solute–solvent interactions and polarisation effects. From Monte Carlo simulations, the structure and energetics of the solutions were determined and solvent effects on the homolytic bond dissociation were analysed.

2 Computational details

Geometry optimisations for the structures of phenol–methanol [PhOH–$(CH_3OH)_{1-2}$] and phenoxy radical–methanol [PhO$^\bullet$–$(CH_3OH)_{1-2}$] clusters were carried out with Becke's three-parameter hybrid exchange functional [20] and the Lee, Yang, and Parr [21] correlation functional (B3LYP). The 6-31 + G(d,p) basis set was used in these optimisations. Single-point energies with the 6-311 + + G(d,p) basis are also reported. To analyse the structure and energetics of OH$^\bullet$–W_N (N = 1–6) clusters, where W is H_2O and N is the number of water molecules, we carried out density functional theory (DFT) ***calculations with the Adamo and Barone [22,23,24] Becke style one-parameter hybrid functional, using a modified Perdew–Wang exchange [24] and PW91 correlation [25] (MPW1PW91). The geometries of OH$^\bullet$-W_N and W_{N+1} clusters (N = 1–6) were fully optimised with Dunning's correlation-consistent polarised-valence double zeta basis set augmented with diffuse functions (aug-cc-pVDZ) [26]. Single-point energy calculations with the aug-cc-pVTZ and aug-cc–pVQZ basis sets [27] are also reported.

The energetics of the clusters with one solute molecule X and N solvent molecules S can be discussed in terms of the binding enthalpies, defined as

$$\Delta H_{b,N} = H[X - S_N] - H[X] - H[S_N], \tag{4}$$

where S_N is a cluster with N solvent molecules. Binding enthalpies $\Delta H_{b,N}$ include zero-point vibrational energy corrections and thermal corrections and were corrected for basis set superposition error (BSSE) by using the counterpoise method [28] with fragment relaxation energy contributions [29].

Monte Carlo simulations were carried out in the isobaric-isothermal (NPT) ensemble [30] at T = 298 K and P = 1 atm. The interactions between two molecules, a and b, were described by a Lennard-Jones (LJ) plus a Coulomb contribution, with parameters ϵ_i, σ_i, and q_i for each atom:

$$U_{ab} = \sum_{i\in a}\sum_{j\in b} 4\epsilon_{ij}\left[\left(\frac{\sigma_{ij}}{r_{ij}}\right)^{12} - \left(\frac{\sigma_{ij}}{r_{ij}}\right)^{6}\right] + \frac{q_i q_j e^2}{r_{ij}}, \tag{5}$$

where $\epsilon_{ij} = (\epsilon_i\epsilon_j)^{1/2}$ and $\sigma_{ij} = (\sigma_i\sigma_j)^{1/2}$.

For the simulations of phenol and the phenoxy radical in methanol, the intermolecular parameters for the interactions between the methanol molecules are from Jorgensen [31]. To describe the solute–solvent interactions we used the LJ parameters of Jorgensen and Nguyen [32]. The solute charges are Merz–Kollman–Singh (MKS) charges [33,34] calculated at the B3LYP/6-31 + G(d,p) level, by using the optimised clusters with two methanol molecules, where the charges of methanol are those corresponding to the intermolecular model.

The simple point charge SPC potential proposed by Berendsen et al. [35] was adopted to represent the interactions between the water molecules. For the hydroxyl radical the LJ parameters are the same as those for the SPC model for water. This procedure is based on the assumption that the LJ parameters are transferable when we move from the parent molecule (water) to the radical species (OH$^\bullet$ radical). Therefore, the main changes in the solute–solvent interactions are related to the polarisation of the solute charge distribution induced by the nearest solvent molecules.

To model the Coulomb interactions between the solute (hydroxyl radical) and the water molecules, the charge distribution of the radical was determined in the OH$^\bullet$–W_5 isomer. The charge distribution of the water molecules in this cluster was represented by SPC charges and a quantum mechanical DFT calculation at the MPW1PW91/aug–cc-pVDZ level was carried out to calculate MKS charges of the OH$^\bullet$ radical. This procedure to estimate the Coulombic solute–solvent interactions takes into account, at least partially, the polarisation of the solute by the closest solvent molecules.

LJ parameters and charge distributions for phenol, the phenoxy radical, and methanol are reported in Table 1. Intermolecular interaction parameters for the OH$^\bullet$ radical and water are reported in Table 2.

The Monte Carlo simulations were carried out with one solute molecule and N = 250 solvent molecules. A cubic cell with periodic boundary conditions was used. The interactions were truncated at a cutoff distance R_c of 12.9 Å (methanol) and 9.6 Å (water). The initial configuration was generated randomly. We carried out $0.5\text{x}10^8$ steps for equilibration. Average values were calculated over $12.5\text{x}10^8$ additional steps. Each step involves the attempt to move one molecule of the system.

From the Monte Carlo simulations, we can estimate solvent effects on the O–H bond dissociation enthalpies for the processes XOH → XO$^\bullet$ + H$^\bullet$, where X is (Ph or H), by using the following equation:

$$D_{sln}(X\text{O–H}) - D(\text{XO}-\text{H}) = \Delta_{sln}H(\text{XO}^\bullet, g) - \Delta_{sln}H(X\text{OH,g}) + \Delta_{sln}H(\text{H}^\bullet, g). \tag{6}$$

This expression can be derived by defining a thermochemical cycle relating gas-phase and solution-phase O–H bond dissociation reactions [1,9]. Solvation enthalpies of the radical species, $\Delta_{sln}H(\text{XO}^\bullet, g)$, and of the parent molecules, $\Delta_{sln}H(\text{XOH,g})$, can be calculated from the simulations [8]. The last term in the Eq. (6) $\Delta_{sln}H(\text{H}^\bullet, \text{g})$, is the solvation enthalpy of the hydrogen atom, which has not been experimentally determined. Usually, it is assumed that it can be approximated by the solvation enthalpy of the hydrogen molecule, $\Delta_{sln}H(\text{H}_2, \text{g})$, which is available in several solvents [1]. Recently, from NPT simulations for H$^\bullet$ in water, we have estimated $\Delta_{sln}H(\text{H}^\bullet, \text{g})$ as –3.8±1.6 kJ/mol [8]. This value is very close to the experimental result for $\Delta_{sln}H(\text{H}_2, \text{g})$ in water (–4.0 kJ/mol) [1]. Here, we assume that both quantities are also similar in methanol. We can also define the difference between the solvation enthalpies of the radical and the parent molecule as

$$\Delta\Delta H = \Delta_{sln}H(\text{XO}^\bullet, \text{g}) - \Delta_{sln}H(\text{XOH,g}). \tag{7}$$

By defining $\Delta D = D_{sln}(\text{XO} - \text{H}) - D(\text{XO} - \text{H})$, we can write

$$\Delta D = \Delta\Delta H + \Delta_{sln}H(\text{H}^\bullet, \text{g}). \tag{8}$$

This expression will be used to discuss solvent effects on the energetics of the O–H bond dissociation enthalpies. We note that when the microsolvation model is used,

$$\Delta\Delta H \approx \Delta\Delta H_N = \Delta H_{b,N}[\text{XO}^\bullet - S_N] - \Delta H_{b,N}[\text{XOH} - S_N] \tag{9}$$

The DFT calculations were carried out with the Gaussian- 98 program [36] and the Monte Carlo simulations with the DICE program [37].

Table 1. Lennard-Jones parameters and charge distribution for phenol, the phenoxy radical, and methanol

Phenol and phenoxy	ϵ (kJ mol^{-1})[a]	σ (Å)	q (au)[b]	
			PhOH	PhO$^{\bullet}$
C1	0.293	3.550	0.5346	0.7151
C2	0.293	3.550	−0.3049	−0.2607
C3	0.293	3.550	−0.3888	−0.3174
C4	0.293	3.550	−0.0910	−0.1051
C5	0.293	3.550	−0.0446	−0.0539
C6	0.293	3.550	−0.2057	−0.1011
H7	0.126	2.420	0.1776	0.1615
H8	0.126	2.420	0.1807	0.2002
H9	0.126	2.420	0.1269	0.1341
H10	0.126	2.420	0.1202	0.1317
H11	0.126	2.420	0.1313	0.1271
O12	0.711	3.070	−0.7399	−0.6315
H13	0.000	0.000	0.5036	
Methanol [c]	ϵ (kJ mol^{-1})	σ (Å)	q(au)	
C1	0.866	3.775	0.265	
H2,H3,H4	0.000	0.000	0.000	
O5	0.711	3.071	−0.700	
H6	0.000	0.000	0.435	

[a] Lennard-Jones parameters from Jorgensen and Nguyen [32]
[b] Merz-Kollman-Singh charges calculated at the 6-31 + G(d,p) level in clusters with two methanol molecules
[c] Interaction parameters from Jorgensen [31]

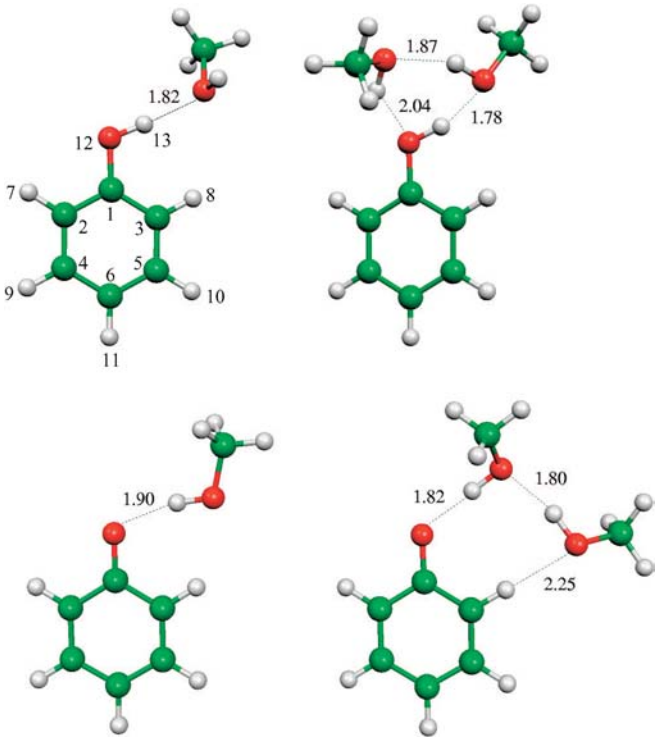

Fig. 1. Structures of the optimised phenol–methanol and phenoxy radical–methanol clusters from B3LYP/6-31 + G(d,p) calculations

Table 2. Lennard-Jones parameters and charge distribution, for the hydroxyl radical and water

OH$^{\bullet}$, H_2O	ϵ (kJ mol^{-1})[a]	σ (Å)[a]	q (au)	
			OH$^{\bullet}$[b]	H_2O[a]
O	0.648	3.165	−0.476	−0.820
H	0.	0.	0.476	0.410

[a] Water single point charge model from Berendsen et al. [35]
[b] Merz–Kollman–Singh charges calculated at the MPW1PW91/aug-cc-pVDZ level in the OH$^{\bullet}$–W_5 complex

3 Phenol O–H homolytic bond dissociation in methanol

3.1 Microsolvation

The optimised structures of phenol–methanol and phenoxy radical–methanol clusters are represented in Fig. 1. These structures illustrate the role played by the phenol molecule as a proton donor (clusters with one and two methanol molecules) and a proton acceptor (cluster with two methanol molecules). This is in contrast with the phenoxy radical, which can only act as proton acceptor in these clusters. When the number of solvent molecules increases in the phenol–methanol clusters we can observe a small reduction of the hydrogen-bond distance between the hydrogen of the phenol O–H group and the methanol oxygen atom: the H...O distance is 1.82 Å in the cluster with one methanol and 1.78 Å in the cluster with two methanol molecules. A small reduction of the distance between the phenoxy radical oxygen and the hydrogen of the methanol O–H group is also observed (Fig. 1). This behaviour (reduction of the hydrogen-bond distances with increasing number of methanol molecules) reflects collective polarisation effects induced by hydrogen bonding and it is quite similar to what is observed in phenol–water and phenoxy radical–water clusters [6].

From single-point-energy calculations at the B3LYP/6-311 + + G(d,p) level with geometries optimised at the B3LYP/6-31 + G(d,p) level, binding enthalpies (for the calculation of $\Delta H_{b,N}$ see Eq. 4) of phenol–methanol clusters are −24.2 (−20.3) kJ/mol for PhOH–CH_3OH and −40.4 (−36.3) kJ/mol for PhOH–$(CH_3OH)_2$, where the values in parentheses are corrected for BSSE. This last value does not include the methanol–methanol interaction energy, which is −24.3 kJ/mol in the free dimer and −20.7 kJ/mol in the geometry of the PhOH–$(CH_3OH)_2$ complex, reflecting the role played by geometric constraints on the energetics of the optimised structures. For phenoxy radical–methanol, $\Delta H_{b,N}$ is −20.8 (−19.2) kJ/mol and −34.8 (−32.0) kJ/mol for PhO$^{\bullet}$–CH_3OH and PhO$^{\bullet}$–$(CH_3OH)_2$, respectively. Therefore, if we adopt the hydrogen-bond-only approach [4], i.e., if we assume that the differential solvation can be estimated by $-\Delta H_{b,N}$(PhOH–CH_3OH) then $\Delta\Delta H$ = 20.3 kJ/mol (see Eq. 7). However, when the solvation of PhO$^{\bullet}$ is considered $\Delta\Delta H$ is significantly lower, i.e., 1.1 kJ/mol (cluster with one methanol molecule) or 4.3 kJ/mol (cluster with two methanol molecules).

Table 3. Energetics of the phenol O–H homolytic bond dissociation in methanol (kJ/mol)

	$\Delta\Delta H_N$ [a]	ΔD_N [b]	$\Delta\Delta H$[c]	ΔD[d]	$\Delta_{sln}H(PhO^{\bullet},g)$	$\Delta_{sln}H(PhOH,g)$
Micro solvation						
Cluster with one CH_3OH	1.1	-2.7 ± 1.6				
Cluster with two CH_3OH	4.3	0.5 ± 1.6				
Monte Carlo			28.1 ± 11	24.3 ± 11	-47.4 ± 7.6	-75.5 ± 7.8

[a] $\Delta\Delta H_N = \Delta H_{b,N}[PhO^{\bullet} - (CH_3OH)_N] - \Delta H_{b,N}[PhOH - (CH_3OH)_N]$
[b] $\Delta D_N = \Delta\Delta H_N + \Delta_{sln}H(H^{\bullet}, g)$, where the solvation enthalpy of the hydrogen atom in methanol was considered similar to the solvation-enthalpy of hydrogen in water (-3.8 ± 1.6 kJ/mol) [8]
[c] $\Delta\Delta H = \Delta_{sln}H(PhO^{\bullet}, g) - \Delta_{sln}H(PhOH, g)$
[d] $\Delta D = \Delta\Delta H + \Delta_{sln}H(H^{\bullet}, g)$

3.2 Monte Carlo simulations

Monte Carlo results for the solvation of phenol and the phenoxy radical in methanol are reported in Table 3. The solvation enthalpy of phenol in methanol was computed as $\Delta_{sln}H(PhOH, g) = -75.5 \pm 7.8$ kJ/mol. This value is similar to our prediction for the hydration enthalpy of phenol (-74.5 ± 6.3 kJ/mol) [8]. It is possibly slightly overestimated owns to the approximation that the phenol molecule has a rigid O–H group [8]. For the phenoxy radical $\Delta_{sln}H(PhO^{\bullet}, g) = -47.4 \pm 7.6$ kJ/mol. Thus, $\Delta\Delta H = \Delta_{sln}H(PhO^{\bullet}, g) - \Delta_{sln}H(PhOH,g)$ is 28.1 ± 11 kJ/mol, indicating, in keeping with our best estimate for the differential hydration enthalpy of phenol and the phenoxy radical [$\Delta\Delta H \equiv \Delta_{hyd}H(PhO^{\bullet}, g) - \Delta_{hyd}H(PhOH,g) = 26.8 \pm 15$ kJ/mol] [8], that the solvent effect is significant and cannot be neglected. Although in this case, the result from the Monte Carlo simulation is in reasonable agreement with the hydrogen-bond-only prediction (20.3 kJ/mol), we believe that this is not, in general, a reliable procedure to predict differential solvation effects.

The radial distribution functions (RDFs) that describe the correlations between the phenol and the phenoxy radical centre-of-mass-positions and the methanol centre-of-mass position are shown in Fig. 2. For the solution with phenol, spherical integration of this function up to the first minimum (6.5 Å), leads to around 15 methanol molecules in the first coordination shell. For the solution with the phenoxy radical, integration up to first minimum (6.9 Å) leads to around 18 methanol molecules (see inset of Fig. 2).

A snapshot of phenol and the phenoxy radical with the first coordination shells is shown in Fig. 3. Although the coordination numbers are nearly the same for both species, the local order related to hydrogen bonding in the two solutions is not equivalent. This is illustrated in Figs. 4 and 5, which describe the correlations related to the role played by phenol as a proton donor (Fig. 4) and phenol and the phenoxy radical as proton acceptors in methanol (Fig. 5). Obviously, the phenoxy radical plays no role as a proton donor in methanol. However, its role as a proton acceptor (Fig. 5) is very similar to the role played by phenol. Thus, it seems reasonable to explain the differential solvation of phenol and the phenoxy radical in a hydrogen-bonding solvent simply by observing that, in these solvents, phenol can act as a good proton donor and acceptor molecule, whereas the phenoxy radical can only accept hydrogen from the solvent.

4 Water O–H homolytic bond dissociation in water

4.1 Microsolvation

The optimised structures of $OH^{\bullet}$–W_N and W_{N+1} clusters are shown in Fig. 6, where the great similarity between them can be observed. One important feature in the $OH^{\bullet}$–W_N clusters is that they reflect the ability of the $OH^{\bullet}$ radical to form hydrogen bonds at both ends. Thus, the $OH^{\bullet}$ radical acts as a proton-donor and proton-acceptor species in a hydrogen-bonding solvent. The structural similarity (Fig. 6) leads, in this case, to energetic similarity, which can be illustrated by comparing binding enthalpies of $OH^{\bullet}$–W_N and W_{N+1} clusters (Fig. 7). $\Delta H_{b,N}$ for the water dimer is -12.3 kJ/mol (MPW1PW91/aug-cc-pVQZ) but the $OH^{\bullet}$–W_1 complex is even stabler than the water dimer ($\Delta H_{b,N} = -17.3$ kJ/mol) . Thus, from the microsolvation results for small clusters, we predict that the differential binding energy of the $OH^{\bullet}$ radical and water is very small, i.e., $\Delta\Delta H_N = -5.0$ kJ/mol (Table 4). A detailed analysis on the structure, vibrational spectrum, and energetics of these clusters has been published elsewhere [38].

For the present system, if we adopt the hydrogen-bond-only approach, (-12.3 kJ/mol) the differential solvation would be overestimated. It is clear that the strong stabilisation of the $OH^{\bullet}$ radical (that can act as a proton donor and proton acceptor) has to be considered explicitly.

4.2 Monte Carlo simulations

The partial RDFs related to hydrogen bonding for the $OH^{\bullet}$ radical solvated in water and pure water are shown in Fig. 8. The $g_{H-O}(r)$ RDF (Fig. 8, left) is related to the role played by the $OH^{\bullet}$ radical as a proton donor in water. This function shows a sharp maximum (2.8 at 1.65 Å). Integration up to the first minimum (0.05 at 2.3 Å) yields 1.0, which is the average number of water oxygen atoms in close interaction with the $OH^{\bullet}$ radical hydrogen. Comparison between $g_{H-O}(r)$ of the hydrated

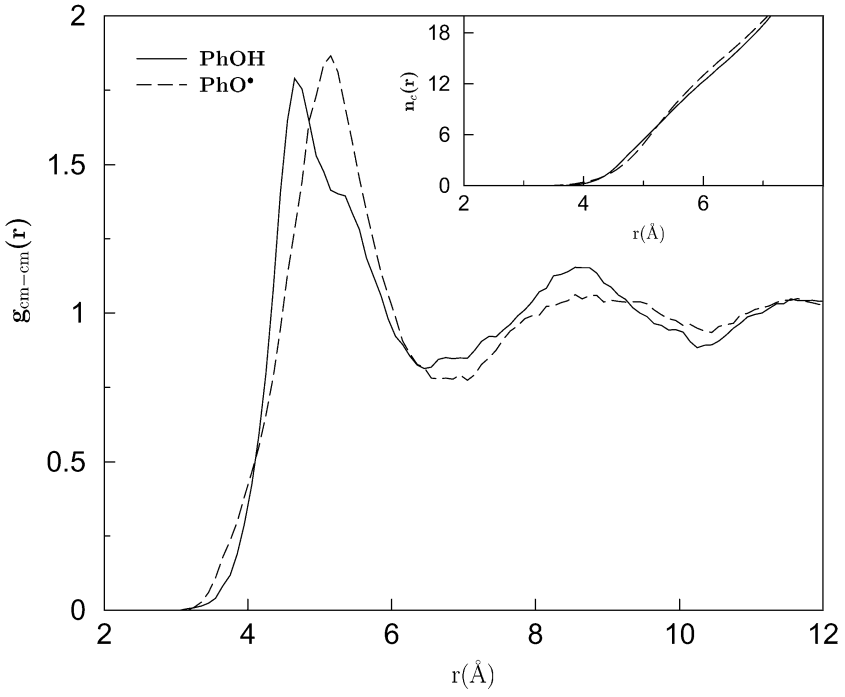

Fig. 2. Partial radial distribution function describing the correlations between the phenol and the phenoxy radical centre- of- mass with the methanol centre- of- mass, $g_{cm-cm}(r)$. The *inset* shows the average coordination number, $n_c(r)$

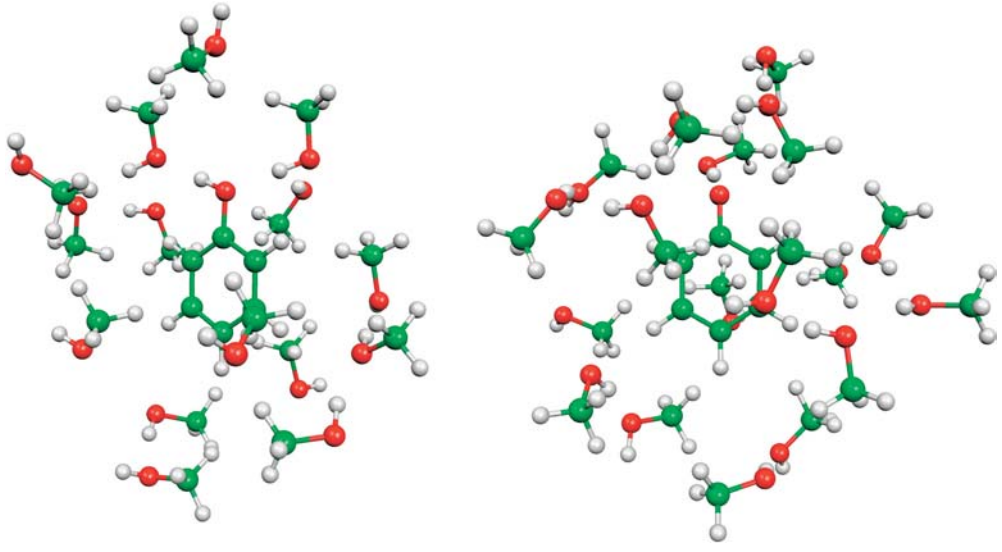

Fig. 3. Snapshot illustrating the structure of the first coordination shell of phenol and the phenoxy radical in methanol

OH• radical and pure liquid water confirms that the short-range order is quite different for the two systems. Moreover, this function illustrates the role that the OH• radical plays as a proton donor in liquid water, which appears to be more significant than the role played by the water molecules as a proton donor in liquid water. The $g_{O-H}(r)$ RDF describes the correlations between the OH• radical oxygen and water hydrogen atoms and illustrates the role played by the OH• radical as a proton acceptor in liquid water. For the hydrated OH• radical this function shows a first maximum (0.6 at 1.9 Å) and integration of this function up to the first minimum (0.42 at 2.3 Å) yields 0.6, which is the average number of hydrogen atoms in close interaction with the OH• oxygen atom. Comparison with the same function for liquid water shows that here the oxygen atom has a stronger interaction with the water hydrogen atoms: $g_{O-H}(r)$ shows a first peak (1.3 at 1.7 Å), and integration up to the first minimum (0.25 at 2.3 Å) yields 0.94.

The energetics results of the water O–H bond dissociation in water are reported in Table 4. We predict that the hydration enthalpy of the OH• radical $\Delta_{sln}H(OH^{\bullet},g) = -39.1\pm4$ kJ/mol. The SPC model predicts that $\Delta_{sln}H(H_2O,g) = -47.9\pm4$ kJ/mol, in good agreement with the experimental value (−44.0 kJ/mol) [39]. Thus, we find that $\Delta\Delta H = \Delta_{sln}H(OH^{\bullet}, g) - \Delta_{sln}H(H_2O, g)$ is 8.8±6 kJ/mol. Consequently, $\Delta\Delta D$ is 5±6 kJ/mol, which indicates that, owing to the stabilisation of the OH• radical, solvent effects on the energetics of HO–H bond in liquid water are quite small.

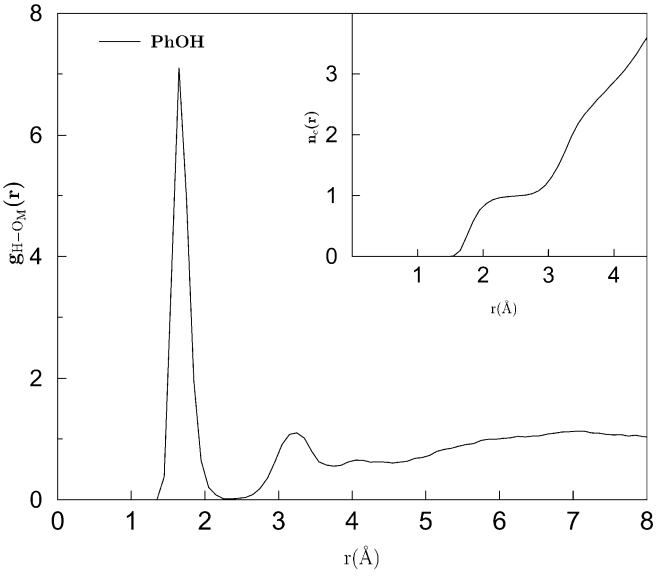

Fig. 4. Partial radial distribution function $g_{H-O}(r)$ for phenol in liquid methanol. The *inset* shows $n_c(r)$

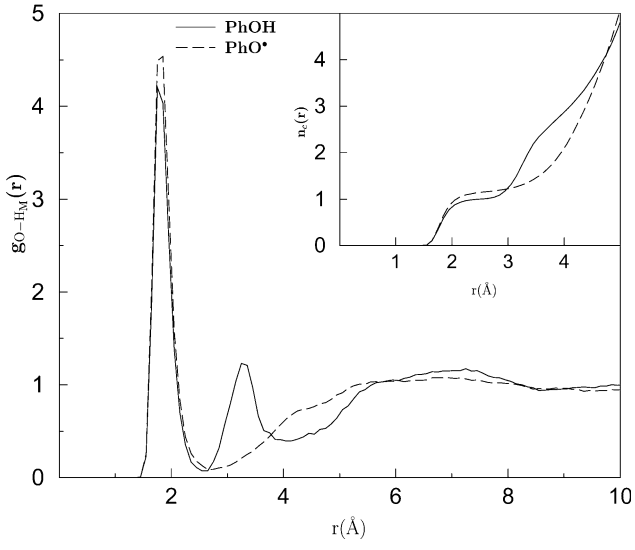

Fig. 5. Partial radial distribution function $g_{O-H}(r)$ for phenol and the phenoxy radical in liquid methanol. The *inset* shows $n_c(r)$

5 Conclusions

This work reports results for the energetics of two O–H bonds in two hydrogen-bonding liquids, methanol and water. Firstly, we analysed the differential solvation of phenol and the phenoxy radical in liquid methanol. From this analysis we have verified that the solvent effect on the energetics of the phenol O–H bond in methanol is significant and that the gas-phase and solution values for the O–H bond dissociation enthalpies differ by around 24 kJ/mol. Our second investigation concerned the energetics of the water O–H bond in water. In this case, we found that the solvent effect on the HO–H bond is quite small (around 5 kJ/mol). This result is related to the strong stabilisation of the OH• radical in water.

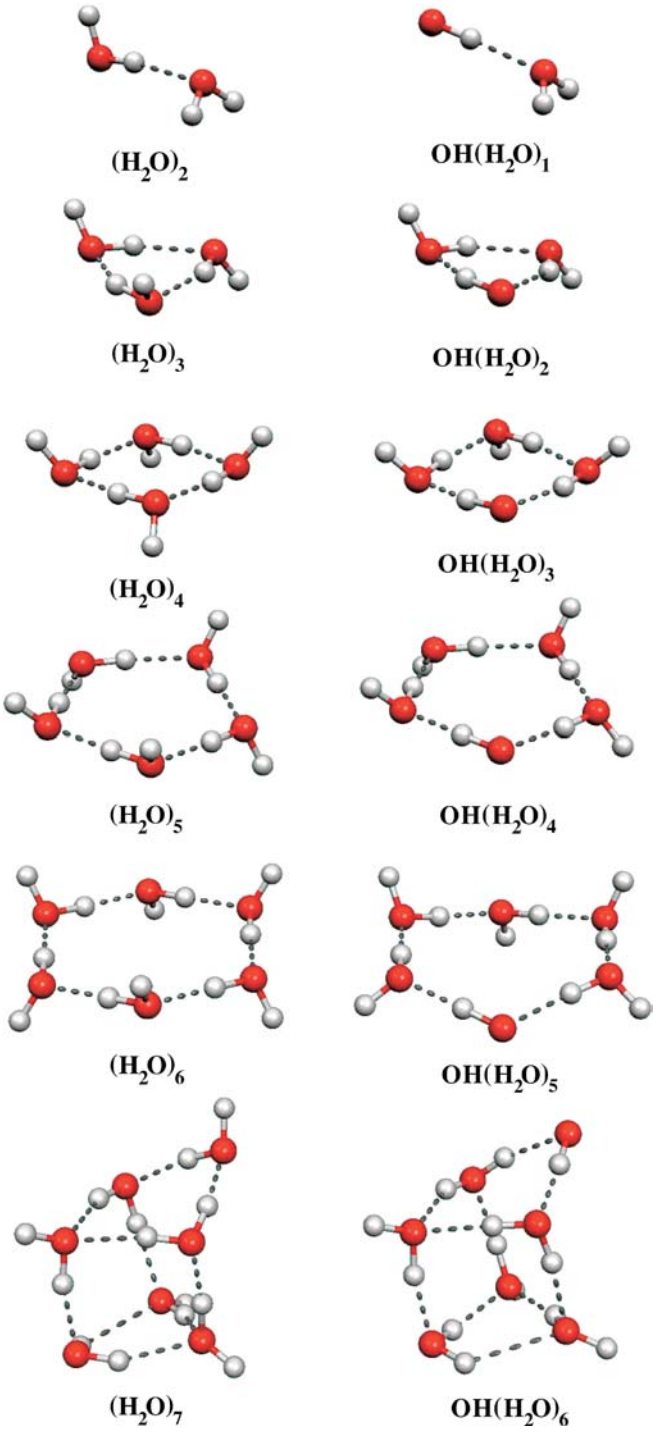

Fig. 6. Optimised structures of water clusters (W_{N+1}) and the hydroxyl radical and water clusters ($OH^{\bullet}$-W_N), from MPW1PW91/aug-cc-pVDZ calculations

Our main conclusion is that to predict solvent effects on the energetics of O–H bonds in an XO–H system it is crucial to correctly estimate $\Delta\Delta H = \Delta_{sln}H(XO^{\bullet}) - \Delta_{sln}H(XO-H)$. We stress the limitations of local models such as microsolvation and hydrogen-bond-only to adequately describe differential solvation effects related to O–H homolytic bond dissociation in hydrogen-bonding liquids.

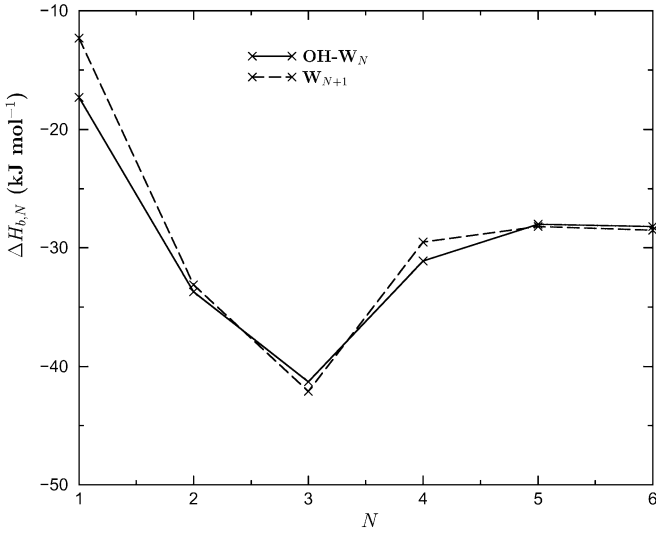

Fig. 7. Binding enthalpies ($\Delta H_{b,N}$) for $OH^{\bullet}$–W_N clusters and for W_{N+1} clusters as a function of N, the number of water molecules in the cluster

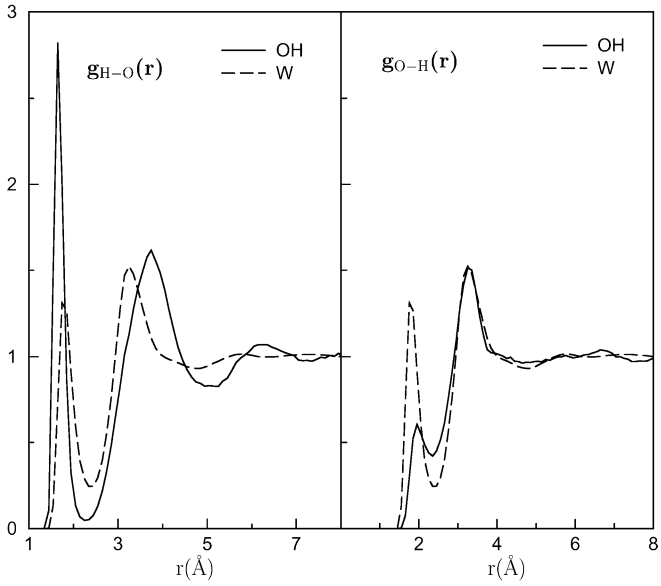

Fig. 8. Partial radial distribution functions $g_{H-O}(r)$ and $g_{O-H}(r)$ for the hydrated $OH^{\bullet}$ radical and for liquid water

Table 4. Energetics of the water O−H homolytic bond dissociation in water (kJ/mol)

	$\Delta\Delta H_N$[a]	ΔD_N[b]	$\Delta\Delta H$[c]	ΔD[d]	$\Delta_{sln}H(OH^{\bullet},g)$	$\Delta_{sln}H(H_2O,g)$
Microsolvation						
Cluster with one H_2O	−5.0	−8.6 ± 1.6				
Cluster with two H_2O	−0.6	−4.4 ± 1.6				
Cluster with three H_2O	0.8	−3.0 ± 1.6				
Cluster with four H_2O	−1.6	−5.4 ± 1.6				
Cluster with five H_2O	0.2	−3.6 ± 1.6				
Cluster with six H_2O	0.3	−3.5 ± 1.6				
Monte Carlo			8.8 ± 6	5 ±6	−39.1 ± 4	−47.9 ± 4

[a] $\Delta\Delta H_N = \Delta H_{b,N}[OH^{\bullet} - W_N] - \Delta H_{b,N}[H_2O - W_N]$
[b] $\Delta D_N = \Delta\Delta H_N + \Delta_{sln}H(H^{\bullet},g)$, where the solvation enthalpy was that of the hydrogen atom in water (−3.8 ±1.6 kJ/mol) [8]
[c] $\Delta\Delta H = \Delta_{sln}H(OH^{\bullet},g) - \Delta_{sln}H(H_2O,g)$
[d] $\Delta D = \Delta\Delta H + \Delta_{sln}H(H^{\bullet},g)$

Acknowledgements. S. G. E., R. C. G. and P. C. dC. gratefully acknowledge the support of Fundação para a Ciência e a Tecnologia. (PhD grants SFRH/BD/10200/2002, PRAXIS/XXI/BD/15920/98, and PRAXIS/XXI/BD/6503/2001). This work was partially supported by the Sapiens program of the FCT, Portugal (grant no. POCTI/43315/QUI/2001).

References

1. Borges dos Santos RM, Martinho Simões JA (1998) J Phys Chem Ref Data 27: 707–739
2. Bordwell FG, Cheng J-P, Harrelson JA Jr (1988) J Am Chem Soc 110: 1229–1231
3. Lind J, Shen X, Eriksen TE, Merenyi G (1990) J Am Chem Soc 112: 479–482
4. Wayner DDM, Lusztyk E, Pagé D, Ingold KU, Mulder P, Laarhoven LJJ, Aldrich HS (1995) J Am Chem Soc 117: 8737–8744
5. Bordwell FG, Liu W-Z (1996) J Am Chem Soc 118: 10819–10823
6. Guedes RC, Costa Cabral BJ, Martinho Simões JA, Diogo HP (2000) J Phys Chem A 104: 6062–6068
7. Cabral do Couto P, Guedes RC, Costa Cabral BJ, Martinho Simões JA (2002) Int J Quantum Chem 86:297–304.
8. Guedes RC, Coutinho K, Costa Cabral BJ, Canuto S (2003) J Phys Chem B 107: 4304–4310
9. Guedes RC, Coutinho K, Costa Cabral BJ, Canuto S, Correia CF, Borges dos Santos RM, Martinho Simões JA (2003) J Phys Chem 107: 9197–9207
10. Weaver EC (1968) Annu Rev Plant Physiol 19: 283
11. Itoh S, Taki M, Fukuzimi S (2000) Coord Chem Rev 198: 3–20
12. Kagan VE, Tyurina YY (1998) Ann N Y Acad Sci 854: 425–434
13. Ruscic B, Feller D, Dixon DA, Peterson KA, Harding LB, Asher RL, Wagner AF (2001) J Phys Chem A 105: 1–4
14. Draganić ZD, Draganić IG (1973) J Phys Chem 77: 765–772
15. Burns WG, Sims HE, Goodall JAB (1983) Int J Radiat Phys Chem 23: 143–163
16. Burns WG (1989) Nature 339: 515–516
17. Jay-Gerin J-P, Ferradini C (2000) Chem Phys Lett 317: 388–291
18. Koppenol WH (1991) Free Radical Biol Med 10: 85–87
19. Aydogan B, Marshall DT, Swarts SG, Turner JE, Boone AJ, Richards NG, Bolch WE (2002) Radiat Res 157: 38–44
20. Becke AD (1993) J Chem Phys 98: 5648–5652
21. Lee C, Yang W, Parr RG (1988) Phys Rev B 37: 785–789
22. Adamo C, Barone V (1997) Chem Phys Lett 274: 242–250
23. Adamo C, Barone V (1998) J Comput Chem 19: 418–429

24. Adamo C, Barone V (1998) J Chem Phys 108: 664–675
25. Perdew JP, Wang Y (1992) Phys Rev B 45: 13244–13249
26. Woon DE, Dunning TH Jr (1993) J Chem Phys 98: 1358–1371
27. Kendall RA, Dunning TH Jr Harrisson RJ (1992) J Chem Phys 96: 6796–6806
28. Boys SF, Bernardi F (1970) Mol Phys 19: 553
29. Xantheas SS (1986) J Chem Phys 104: 8821–8824
30. Frenkel D, Smit B (1996) Understanding molecular simulation Academic San Diego
31. W. L. Jorgensen, J Phys Chem (1986) 90:1276–1284.
32. Jorgensen WL, Nguyen TB (1993) J Comput Chem 14: 195–205
33. Singh UC, Kollman PA (1984) J Comput Chem 5: 129–145
34. Besler BH, Merz KM Jr, Kollman PA (1990) J Comput Chem 11: 431–439
35. Berendsen HJC, Postma JPM, van Gusteren WF, Hermans J (1981) In:Pullman B (ed) Intermolecular Forces. Reidel, Dordrecht, p 331
36. Frisch MJ, Trucks GW, Schlegel HB, Scuseria GE, Robb MA, Cheeseman JR, Zakrzewski VG, Montgomery JA, Stratman RE, Burant JC, Dapprich S, Millan JM, Daniels AD, Nudin KN, Strain MC, Farkas O, Tomasi J, Barone V, Cossi M, Cammi R, Mennucci B, Pomelli C, Adamo C, Clifford S, Ochterski J, Peterson GA, Ayala PY, Cui Q, Morokuma K, Malick DK Rabuck AD, Raghavachari K, Foresman JB, Cioslowski J, Ortiz JV, Stefanov BB, Liu G, Liashenko A, Piskorz P, Komaromi I, Gomperts R, Martin RL, Fox DJ, Keith T, Al-Laham MA Peng CY, Nanayakkara A, Gonzalez C, Challacombe M, Gill PMW, Johnson BG, Chen W, Wong MW, Andres JL, Head-Gordon M, Repogle ES, Pople JA (1998) GAUSSIAN- 98. Gaussian Pittsburgh, PA
37. Coutinho K, Canuto S (2000) DICE: A general Monte Carlo program for liquid simulation. University of São Paulo, Brazil
38. Cabral do Couto P, Guedes RC, Costa Cabral BJ, Martinho Simões JA (2003) J Chem Phys 119: 7344–7354
39. Cox JD, Wagman DD, Medvedev VA (eds) (1989) CODATA key values for thermodynamics. Hemisphere, New York